

Optical characterization of a dual-frequency hybrid aligned nematic liquid crystal cell

S. A. Jewell and J. R. Sambles

Thin Film Photonics Group, School of Physics, University of Exeter, Stocker Road, Exeter, EX4 4QL, England
s.a.jewell@exeter.ac.uk

Abstract: The dielectric anisotropy of a highly dispersive dual-frequency nematic liquid crystal (MDA-00-3969 (Merck KGa)) has been determined using the optical fully-leaky guided-mode technique. A $4V_{\text{rms}}$ sinusoidal voltage was applied across a $5\mu\text{m}$ hybrid aligned nematic (HAN) cell at various frequencies in both the positive and negative dielectric anisotropy regime. Optical data was collected at each frequency enabling the director profile in each case to be determined using a multi-layer optics model in combination with a liquid crystal free-energy minimization routine. The thresholdless response of the HAN cell combined with the extreme sensitivity of the optical characterization technique has allowed subtle changes in dielectric permittivity with frequency to be observed. The resulting measured dispersion shows excellent agreement with a single Debye-type relaxation model.

© 2005 Optical Society of America

OCIS codes: (160.3710) Liquid crystals; (310.3840) Materials and process characterization)

References and links

1. G.P. Bryan-Brown, C.V. Brown, I.C. Sage, V.C. Hui, "Voltage-dependent anchoring of a nematic liquid crystal on a grating surface" *Nature* **392**, (6674) 365 (1998)
2. S. Kitson and A. Geisow, "Controllable alignment of nematic liquid crystals around microscopic posts: Stabilization of multiple states" *Appl. Phys. Lett.* **80**, (19) (2002)
3. E.P. Raynes and I. Shanks, "Fast switching twisted nematic electro-optical shutter and colour filter," *Electron. Lett.* **10**, 114 (1974)
4. M. Schadt, "Liquid crystal materials and liquid crystal displays," *Annu. Rev. Mater. Sci.* **27**, 305 (1997)
5. S.A. Jewell and J.R. Sambles, "Fully leaky guided mode study of the flexoelectric effect and surface polarization in hybrid aligned nematic cells," *J. Appl. Phys.* **92**, (1) 19 (2002)
6. Y.Q. Lu, X. Liang, Y.H. Wu et. al, "Dual-frequency addressed hybrid-aligned nematic liquid crystal," *Appl. Phys. Lett.* **85**, (16) 3354 (2004)
7. S.A. Jewell and J.R. Sambles, "Observation of backflow in the switch-on dynamics of a hybrid aligned nematic," *Appl. Phys. Lett.* **84**, (1) 46 (2004).
8. P.G. De Gennes, "The Physics Of Liquid Crystals," Clarendon, Oxford (1974)
9. S.A. Jewell and J.R. Sambles, "Fully-leaky guided-mode measurement of the flexoelectric constant ($\epsilon_{11}+\epsilon_{33}$) of a nematic liquid crystal," *Mol. Cryst. Liq. Cryst.* **401**, 181
10. F. Yang, L. Ruan and J.R. Sambles, "Homeotropic polar anchoring energy of a nematic liquid crystal using the fully leaky waveguide technique," *J Appl Phys* **88**, (11) 6175 (2000)
11. F. Yang, J.R. Sambles, Y.M. Dong and H. Gao, "Fully leaky guided wave determination of the polar anchoring energy of a homogeneously aligned nematic liquid crystal," *J Appl Phys* **87**, 2726 (2000)
12. D.Y.K. Ko and J.R. Sambles, "Scattering matrix method for propagation of radiation in stratified media: attenuated total reflection studies of liquid crystals," *J. Opt. Soc. Am. A.* **5**, 1863 (1988)
13. M. Schadt, "Kerr effect and orientation relaxation of pretransitional domains and individual molecules in positive dielectric liquid crystals," *J. Chem. Phys.* **67**, 210 (1977)

1. Introduction

Dual-mode liquid crystal displays offer the potential to operate in either a low-power black and white reflective bistable mode for displaying simple, low resolution data or in a colour high-resolution emissive mode for the display of video-rate images. However, the relatively

slow switching speed of current monochrome bistable displays, such as the ZBD¹ and PABN² devices, hinders their application in a dual-mode device. In these bistable devices two optically different states are produced by the director changing alignment at one of the surfaces resulting in two different stable configurations being permitted. The associated switching speed is governed by the mechanical and viscous properties of the liquid crystal material. An alternative way of switching a liquid crystal device between two states is to use a dual-frequency nematic liquid crystal^{3,4}. Such materials have dielectric anisotropies which are highly dependent on the frequency of the applied field; $\Delta\epsilon (= \epsilon_{//} - \epsilon_{\perp})$ can be positive, negative or zero, depending on the frequency chosen. In particular, liquid crystal compounds are available where the dielectric permittivity is highly dispersive, resulting in the dielectric anisotropy actually changing sign at a particular frequency referred to as the cross-over frequency, f_{co} . These materials can therefore be driven into an alignment either parallel or perpendicular to the direction of the applied field by simply modifying the frequency of the field applied. Dispersion in a liquid crystal is dependent on the molecular structure, viscosity and temperature of the material. It arises due to the molecular rotation about the short axis being hindered in the nematic phase resulting in the value of $\epsilon_{//}$ varying with the frequency of the applied field. Conversely, the rotation about the long axis of the uniaxial molecule is unrestricted and ϵ_{\perp} is almost constant up to GHz frequencies. Dual-frequency liquid crystal materials are mixtures of several highly dispersive positive and negative dielectrically anisotropic materials combined to produce a compound with a dielectric anisotropy ranging from positive at low frequencies to negative at high frequencies.

The facility to drive such a material into either homeotropic or homogeneous alignment lends itself to the hybrid aligned nematic (HAN) structure. A HAN cell has homogeneous alignment (parallel to the substrate) on one surface, and homeotropic alignment (perpendicular to the surface) on the other. In the absence of any chiral dopant in the liquid crystal, the director will tilt through approximately 90° from one surface to the other, giving a near-linear variation in tilt with distance across the cell⁵. To a first approximation, the HAN structure has an equal bias towards both homogeneous and homeotropic alignment, and so when a voltage is applied across the cell, the director will readily respond by either aligning with or perpendicular to the field depending on the frequency applied. This results in the cell effectively having three stable states, one at 0V, governed primarily by the elastic constants of the material and the other two being homogeneous or homeotropic alignment which is maintained whilst an electric field of a suitable frequency is applied across the cell⁶. In particular, the HAN structure has no threshold voltage and so will respond to small changes in the dielectric free-energy of the system produced by the application of a voltage at frequencies where the dielectric anisotropy is very small. This makes the structure ideal for studying the fundamental properties of these dual frequency materials. Furthermore, dynamic studies of HAN cells have demonstrated that they have a switch-on time of a few milliseconds, and hence show a great potential for fast-switching applications⁷, although their considerably longer switch-off time hinders their use in practical devices. By combining this structure with a dual-frequency material, the director can therefore be rapidly driven between the homogeneous and homeotropic alignments.

By measuring the director profile in a dual-frequency HAN cell when voltages are applied at a range of frequencies, it is possible to determine the dielectric permittivity at each frequency by comparing the measured profile with theoretical profiles generated by minimising the free-energy of the system⁸. This is given by the sum of the elastic and dielectric free-energy densities of the system:

$$G = \int_0^d \left[\frac{1}{2} (K_{11} (\mathbf{n} \cdot \nabla \cdot \mathbf{n})^2 + K_{22} (\mathbf{n} \cdot (\nabla \times \mathbf{n}))^2 + K_{33} (\mathbf{n} \times \nabla \times \mathbf{n})^2) + \frac{1}{2} \mathbf{D} \cdot \mathbf{E} \right] dz \quad (1)$$

where K_{11} , K_{22} and K_{33} are the splay, twist and bend elastic constants respectively, \mathbf{D} is the displacement field and \mathbf{E} is the electric field where $\mathbf{D} = \epsilon_0 \underline{\epsilon} \mathbf{E}$. For a non-twisted HAN cell of

thickness d , $\frac{\partial}{\partial x} = \frac{\partial}{\partial y} = 0$ and the x and z components of the director are given by

$n_x = \sin \theta$ and $n_z = \cos \theta$ where θ is the tilt angle measured from the normal to the substrate. For a voltage applied across the liquid crystal layer (in the z -direction) $D_x = D_y = E_x = E_y = 0$ and, from Maxwell's equations:

$$D_z = \epsilon_0 (\Delta \epsilon(f) \sin^2 \theta + \epsilon_{\perp}) E_z(z) \quad (2)$$

where D_z is continuous through the cell. The free-energy expression therefore becomes⁸:

$$G = \frac{1}{2} \int_0^d \left[(K_{11} \sin^2 \theta + K_{33} \cos^2 \theta) \left(\frac{d\theta}{dz} \right)^2 + \frac{D_z^2}{\epsilon_0 (\epsilon_{\parallel}(f) \cos^2 \theta + \epsilon_{\perp} \sin^2 \theta)} \right] dz \quad (3)$$

At the cross-over frequency, f_{co} where $\epsilon_{\parallel}(f_{co}) = \epsilon_{\perp}$ the dielectric contribution to the free energy is constant and hence, to a first approximation, neglecting heating effects, it is independent of the applied field. The director profile in the HAN cell is thus dictated by the elastic free-energy and therefore retains its near-linear profile associated with the 0V equilibrium profile.

To allow a successful comparison between theoretical and measured profiles the director profile must be determined with a high degree of accuracy. One such characterization method which is suited to such an application is the optical fully-leaky guided-mode technique^{10,11}. This well-established method has been used to determine the director structure in a range of liquid crystal cells, and involves collecting optical intensity versus angle-of-incidence data from the cell, and comparing it to model data generated using a multi-layer optics model. This method has an excellent sensitivity to subtle changes in the optical properties of the liquid crystal layer, produced by the reorientation of the liquid crystal director. It is therefore ideal for detecting the changes in the director orientation that occurs when the dielectric anisotropy is changed by a small amount, by adjusting the frequency of the applied field.

2. Experiment

A 5 μ m HAN cell containing the dual-frequency nematic liquid crystal MDA-00-3969 (Merck KGaA) was constructed using two glass plates of refractive index $n = 1.52$ coated in a 30 nm layer of ITO to provide a transparent electrode. The substrate was treated with a monolayer of octadecyltrimethoxysilane (OTMS) to produce homeotropic alignment at the lower interface, and a 60 nm layer of polyimide was deposited on top of the ITO layer of the superstrate and rubbed to promote homogeneous alignment. The cell was spaced using 5 μ m beads dispersed in UV setting glue and filled by capillary flow with the liquid crystal in the isotropic phase.

To obtain the optical intensity versus angle-of-incidence data, the cell was index-matched between two glass prisms ($n = 1.52$) and mounted at the centre of a computer-controlled rotating table (Fig. 1). Light from a 5mW Helium-Neon laser ($\lambda = 632.8$ nm) was passed through a polarizer to select either p - (transverse magnetic) or s - (transverse electric) polarized light and was then incident on the prism and cell arrangement.

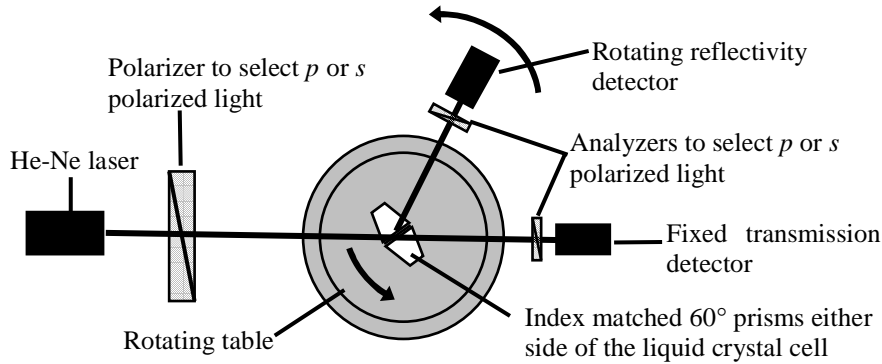


Fig. 1. Schematic diagram of the layout of the apparatus used in the fully-leaky guided-mode optical characterization technique.

For each angle of incidence, the intensity of the p - and s - components of the transmitted and reflected beams were collected, with 8 polarization datasets collected in total, 4 in transmission (p - p and s - s conserving and p - s and s - p converting) and the same 4 combinations in reflection. This process was repeated numerous times with a $4V_{\text{rms}}$ a.c. voltage applied across the cell at different frequencies in the range from 1 kHz to 64 kHz. (This voltage was chosen as it produced a good variety of director distortions over the chosen frequency range.) To determine the director profile at each frequency, the optical data were normalised and fitted to using a multi-layer optical model based on a 4×4 Berreman matrix¹² using a least-squares fitting procedure. The fitting parameters included the optical permittivities, absorption and thickness of the ITO, polyimide and liquid crystal. The director profile and hence the optical properties of the liquid crystal layer were modelled using a free-energy minimization model with the physical constants of the material (the elastic constants K_{11} and K_{33} , the dielectric permittivity ϵ_{\perp} and dielectric anisotropy $\Delta\epsilon(f)$), the surface anchoring and the applied voltage being used as fitting parameters. The optical data for each applied frequency was fitted to independently, with all of the parameters allowed to vary, allowing the mean value for each of the parameters to be determined and the uncertainty in these values to be ascertained.

3. Results and discussion

Figure 2 shows examples of polarization conversion (p - to s - polarized) optical data collected in reflection and transmission. As the frequency of the applied field is increased from 1kHz up to the cross-over frequency (Fig. 2(a)) a clear trend can be seen as the general level of polarization conversion increases which arises due to the director reorientating from the predominantly homeotropic alignment through the cell. Figure 2(b) shows the optical data collected as the frequency is increased further from the crossover frequency into the negative dielectric regime. In this case the director changes from the Maugin polarization-guiding linear director variation to the near homogeneously aligned and hence birefringent state.

A selection of the tilt profiles produced from the optical fits are shown in Fig. 3. The tilt profiles were produced for each frequency with $K_{33}/K_{11} = 1.4 \pm 0.1$ determined from the fitting procedure. This is a typical value for the splay-bend elastic constant ratio (no precise values were available for this material from the manufacturer). A surface anchoring value of $1 \times 10^{-5} \text{ Jm}^{-2}$ was used for both surfaces in the director modelling routine and this suggests reasonably strong anchoring at both the homogeneous and homeotropic surfaces. As expected the homogeneous surface tilt decreases as the dielectric anisotropy becomes increasingly positive, and the homeotropic surface tilt increases with the dielectric anisotropy becoming increasingly negative.

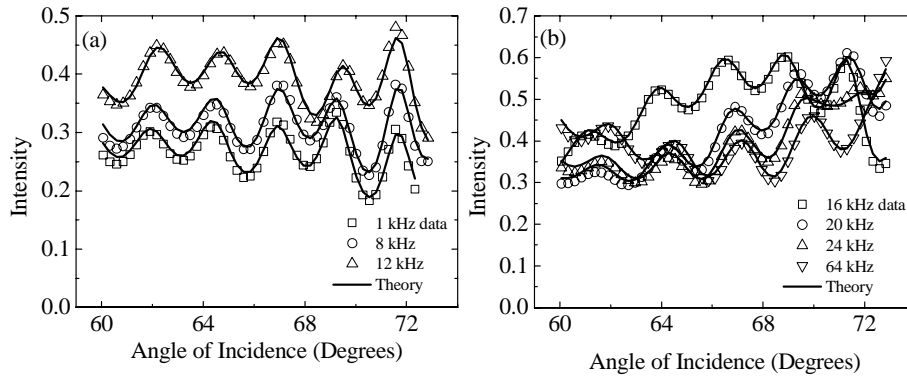


Fig. 2. Some of the optical fully-leaky guided mode data collected at the frequencies indicated (symbols) and the theoretical data generated using a multi-layer optics model and least-squares fitting procedure (lines) for *p*- to *s*-polarization converting transmitted light.

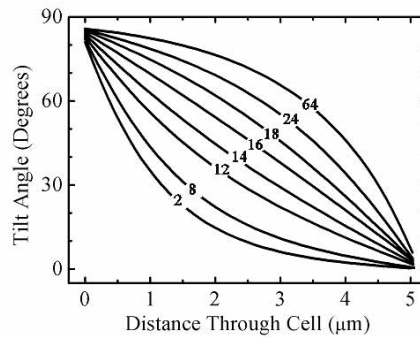


Fig. 3. Measured director profiles at a selection of applied frequencies (shown in kHz) for the variation in the tilt angle of the director (measured from the normal to the substrate) with distance through the cell.

Figure 4 shows the values of the dielectric anisotropy determined through the fitting procedure plotted as a function of frequency and, by interpolation, the crossover frequency at this temperature (19.5°C) is determined as 13.0 (±0.2) kHz. Fitting to the optical data revealed that the director profile was relatively insensitive to the absolute values of the parallel and perpendicular permittivities with the dielectric anisotropy being the most significant fitting parameter. As a result the value of the perpendicular anisotropy (believed to be frequency independent over the frequency range used) was held at $\epsilon_{\perp}=6$, which tended to give the best results during the preliminary fitting stages, and only $\Delta\epsilon(f)$ was varied during the final fitting procedure.

The variation of ϵ_{\parallel} with frequency can be described by a single, Debye type relaxation model¹³ of the form:

$$\epsilon_{\parallel}(f) = \epsilon_{\parallel}(\infty) + \frac{\epsilon_{\parallel}(0) - \epsilon_{\parallel}(\infty)}{1 + f^2 \tau_o^2} \quad (4)$$

where $\epsilon_{\parallel}(0)$ and $\epsilon_{\parallel}(\infty)$ are the static and high-frequency values of the parallel permittivity and τ_o is the Debye relaxation time.

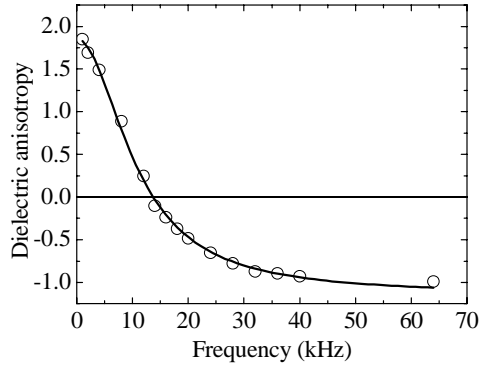


Fig. 4. The variation of the measured dielectric anisotropies (symbols) with frequency determined by fitting to the optical data and the fit to a single Debye-type relaxation (line).

Assuming that ϵ_{\perp} is constant over the frequency range used, Eq. (4) can be written in terms of the dielectric anisotropy of the material in the form:

$$\Delta\epsilon(f) = \Delta\epsilon(\infty) + \frac{\Delta\epsilon(0) - \Delta\epsilon(\infty)}{1 + f^2 \tau_o^2} \quad (5)$$

The result of fitting this expression to the measured variation of dielectric anisotropy with frequency is shown in Fig. 4 using $\Delta\epsilon(\infty) = -1.15 (\pm 0.03)$, $\Delta\epsilon(0) = +1.85 (\pm 0.03)$ and the Debye relaxation time $\tau_o = 93 (\pm 3) \mu\text{s}$. From these parameters, a model value of the cross-over frequency, f_{co} can be determined by using $\Delta\epsilon(f_{co}) = 0$ in Eq. (5) to give the expression:

$$f_{co} = \frac{1}{\tau_o} \left(\frac{\Delta\epsilon(0)}{|\Delta\epsilon(\infty)|} \right)^{\frac{1}{2}} \quad (6)$$

Using the values for $\Delta\epsilon(\infty)$, $\Delta\epsilon(0)$ and τ_o obtained from the fitting procedure gives the cross-over frequency as $13.7 (\pm 0.4) \text{ kHz}$ which agrees well with the value suggested from the dielectric anisotropy measurements. However, some slight discrepancy arises between theory and experiment around this region possibly due to dielectric heating occurring in the material. The complex dielectric permittivity of the liquid crystal along the long axis is of the form $\epsilon_{\parallel}^*(f) = \epsilon'_{\parallel}(f) + i\epsilon''_{\parallel}(f)$ where the real part, $\epsilon'_{\parallel}(f)$, is given by Eq. (4) and the imaginary part is ⁴:

$$\epsilon''_{\parallel}(f) = \frac{\epsilon_{\parallel}(0) - \epsilon_{\parallel}(\infty) f \tau_o}{(1 + f^2 \tau_o^2)} \quad (7)$$

The dielectric dissipation of the material, which generates heat, is governed by the imaginary component of the complex dielectric permittivity and is a maximum at the Debye relaxation

frequency, $f_o = 1 / \tau_o$ which in the case of the measured material, is 10.8 (\pm 0.3) kHz. At this frequency, maximum heating of the liquid crystal occurs. Due to the high variation of the dielectric permittivity with temperature (arising through its intrinsic dependence on the order parameter, S , of the compound) measurements taken of the dielectric anisotropy close to this frequency are liable to have a higher degree of error associated with them, despite reasonable steps being taken during the characterization process to maintain the cell at a constant temperature. This is suggested in the slight difference between the measured dielectric anisotropy and the Debye model fit around $f=10.8$ kHz in Fig. 4, although more data in this region would be required to confirm this.

4. Conclusion

The optical fully-leaky guided-mode technique has been used to accurately measure the frequency dependent director tilt profiles in a 5 μ m HAN cell filled with the dual-frequency nematic material MDA-00-3969. By using a free-energy minimization model the dielectric anisotropy of the material at frequencies above and below the cross-over frequency have been determined. The resulting variation of the dielectric anisotropy with frequency agrees well with a single Debye-type relaxation model and the cross-over frequency calculated agrees with that observed experimentally.

Acknowledgments

The authors would like to acknowledge funding from the EPSRC as part of a Faraday COMIT partnership and would like to thank Dr I R Hooper for the development of the liquid crystal modelling code.